Kaymazlar, Andac, Garcia, Support Information for "Healable, Recyclable and Universal Reversible Underwater Solid-Adhesive" submitted to Journal of Materials Chemistry A, 2024.

Supporting Information for:

Water-triggered self-healing and reversible underwater adhesion in metalorganic polymers

Elif Kaymazlar, Omer Andac, Santiago J. Garcia*

***Corresponding author**

Santiago J. Garcia Email address: S.J.GarciaEspallargas@tudelft.nl

Experimental Section

Materials

Bis(3-aminopropyl) terminated poly(dimethylsiloxane) (NH_2-PDMS-NH_2) with an average Mw=5000 g/mol was purchased from abcr Gute Chemie. Dichloromethane (DCM, 99%), 2,5-thiophenedicarboxyaldehide, ferric chloride zinc acetate, and nickel nitrate were purchased from Sigma Aldrich. All of the chemicals were used as received.

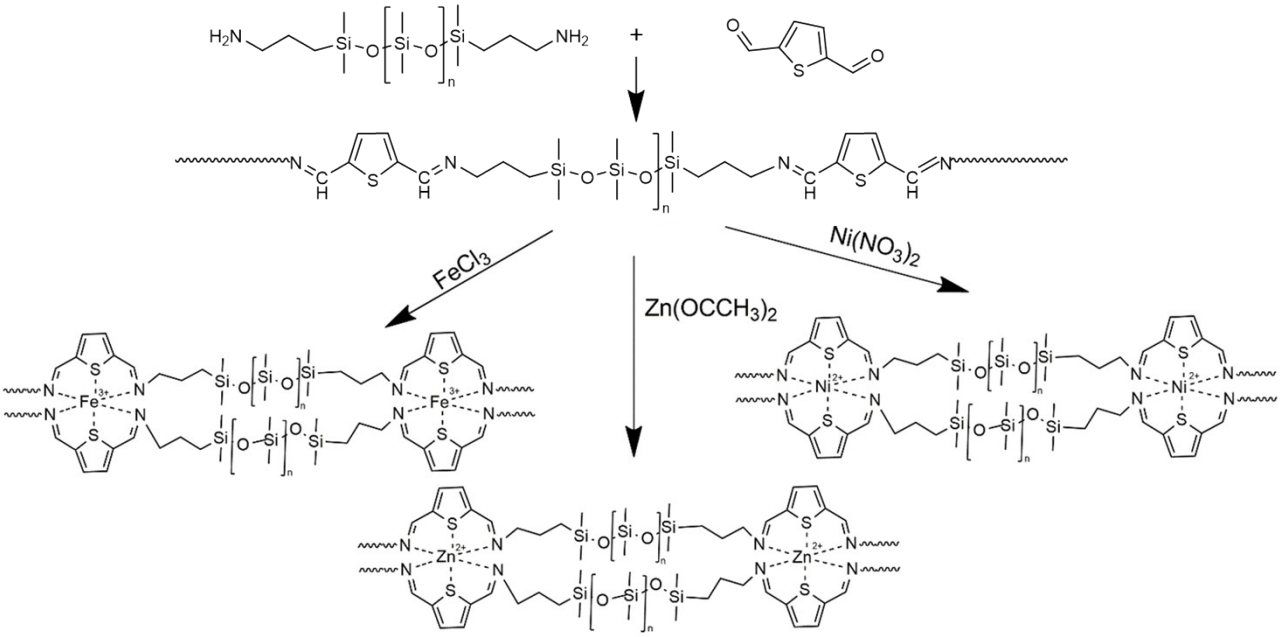

Figure S1. Schematic route of synthesis reversible, healable and recyclable adhesive elastomer.

Quantum chemical calculation of coordination bond energies

The metal complexes were analyzed using “Gaussian16” commercial software. The model structures were calculated using Density Functional Theory (DFT) with the B3LYP method in Gaussian16. The calculations utilized the 6-311+G(2d-2p) basis set for non-metal atoms and LANL2DZ for the metal atoms. Geometric optimizations of complexes were carried out for both low- spin and high- spin states. Spin multiplicity is taken as 6 for iron and 3 for nickel for high- spin state, and 2 for iron and 1 for nickel for low- spin state. As zinc complexes have only one spin multiplicity value due to filled d orbitals, multiplicity is taken as 1 for calculating zinc complexes. The high spin complex of QTFe and the low spin complex of QTNi were shown to be more stable. Consequently, coordination bond energies were calculated using these stable complexes. The coordination bond energies were calculated using Eq. S1 and Eq. S2 according to the bond valence-bond length correlation[1], derived from the obtained bond lengths.

$$E = aS^2 \qquad \text{(Eq. S1)}$$

$$S = \exp((R_0 - R)/b) \qquad \text{(Eq. S2)}$$

Here, "a" is a constant with a value of 7 eV vu-2. "R" represents the observed bond length, while "R0" and "b" are theoretical bond valence parameters obtained from theoretical calculations[1, 2].

Cross-linking density calculations

The crosslinking density of polymers was calculated via swelling tests according to Flory-Rehner equation[3] (Eq. S3). The polymers were immersed in toluene for 3 days until equilibrium between polymer and solvent was breached. To calculate crosslinking density, and following previous literature reports, it was assumed that the dynamic cross-links are not affected by the solvent in the immersion timeframe.

$$\ln(1-V_r)+V_r+\chi V_r^2 = -\frac{\rho}{Mc}V_s\left(V_r^{1/3} - \frac{2Vr}{f}\right) \qquad \text{(Eq. S3)}$$

Where:

V_r= volume fraction of swollen polymer

χ= polymer-solvent interaction parameter (0.465 for PDMS-toluene)

ρ_r= polymer density

M_c= molecular weight of polymer between two crosslinks

V_s= molar volume of solvent (106.5 mL/mol for toluene)

f= functional crosslinks (6 for all complexes)

The volume fraction (V_r) of swollen polymer was calculated according to Eq. S4:

$$V_r = \frac{Wi/\rho r}{\frac{Wi}{\rho r} + (Ws - Wd)/\rho s} \quad \text{(Eq. S4)}$$

Where:

w_i= initial weight of the sample

w_s= swollen weight of the sample

w_d= weight of the dried sample after evaporation of the solvent

ρ_s= solvent density (0.865 g/cm^3 for toluene)

The crosslinking density (v) is calculated as:

$$v = \frac{1}{2Mc}$$

Table S1. Molecular weight of polymer between two crosslinks (Mc) and crosslinking density (v) of the synthesized samples

Samples	**Mc x10^4 (g/mol)**	**v x10^{-6} (mol/g)**
QTFe	1.4 ± 0.9	34.9 ± 0.23
QTNi	3.4 ± 0.18	14.8 ± 0.08
QTZn	29.5 ± 2.1	1.6 ± 0.11

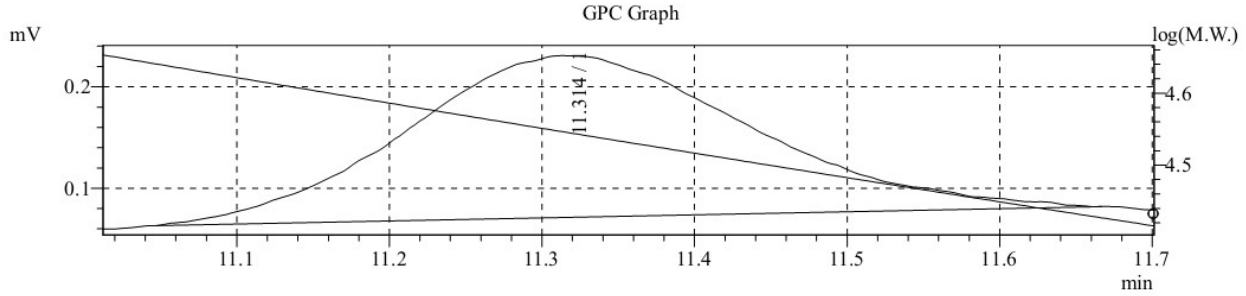

Fig. S2 GPC elution curves of QT (2,5-thiophenedicarboxyaldehyde-PDMS Schiff base). Molecular weight and molecular weight distributions were calculated according to calibration using a series of poly(methyl methacrylate) (PMMA) standards (Mn=625-29400 g/mol).

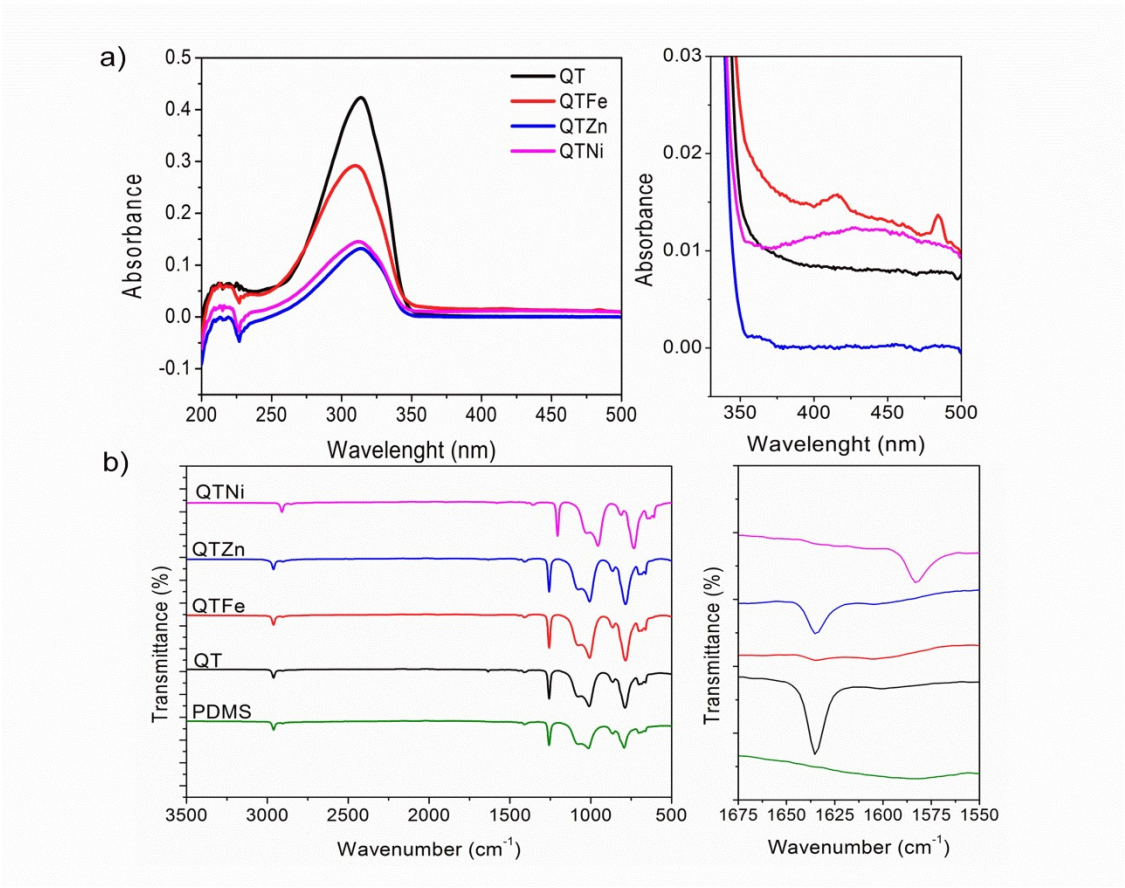

Fig. S3 Polymer characterization with UV and IR: (a) UV-Vis spectra of polymers, enlarged region 345-500 nm range was chosen to identify details related to metal complexes. The absorbance band at 317 nm represent π-π* transition of imine bond; (b) FT-IR spectra of polymers, enlarged region 1650- 1550 cm^{-1} range was chosen to identify details related to imine bonds. The characteristic peaks of imine bond were observed at 1634 cm^{-1} for QT and the peak shifted to a different wavenumber after complexation.

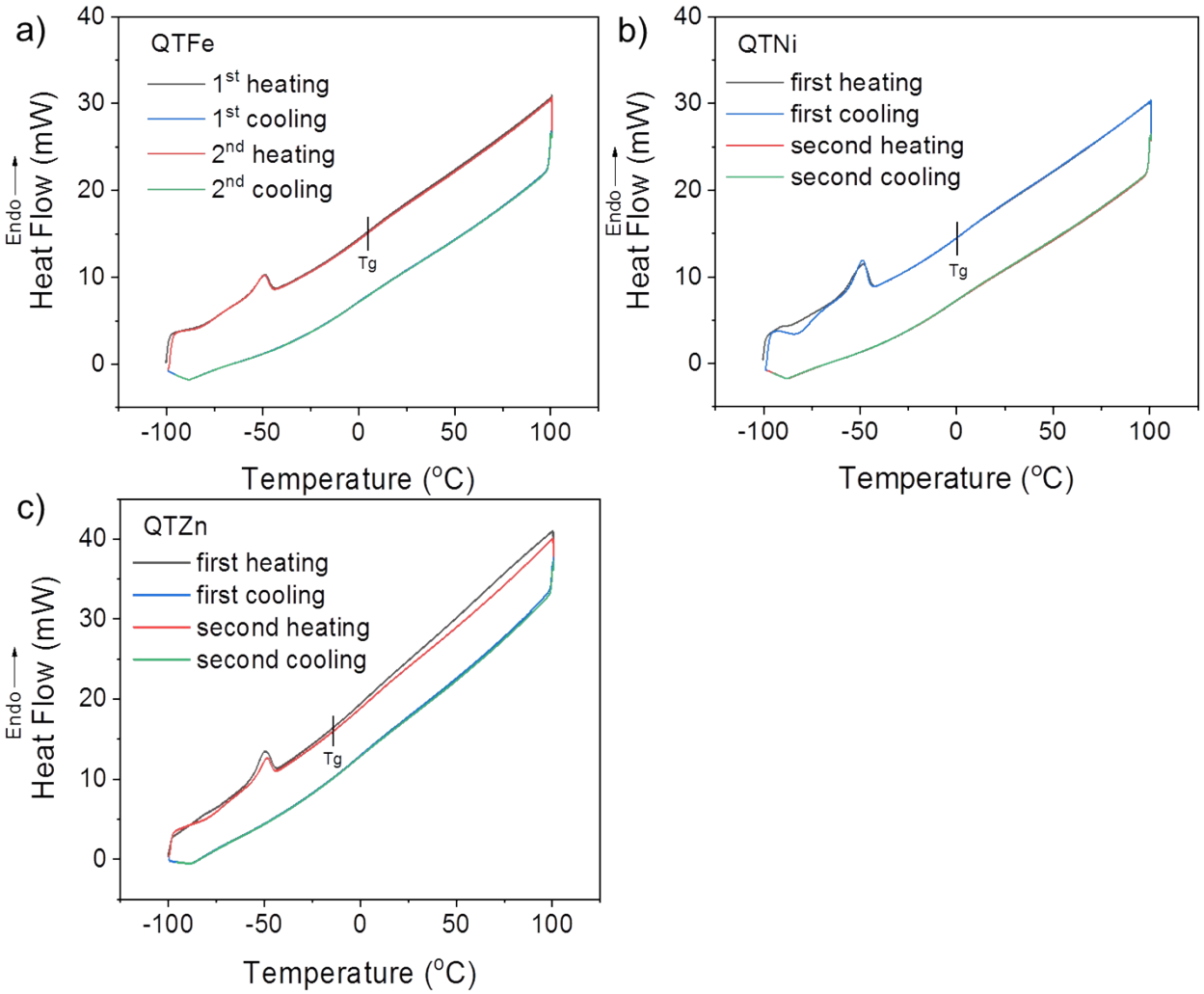

Fig. S4 The DSC curves for: a) QTFe, b) QTNi; and c) QTZn. An endothermic peak around -50 °C corresponded to melting is observed. The midpoint Tg of the polymers was at approximately 5°C, -1°C and -14°C, respectively.

a)

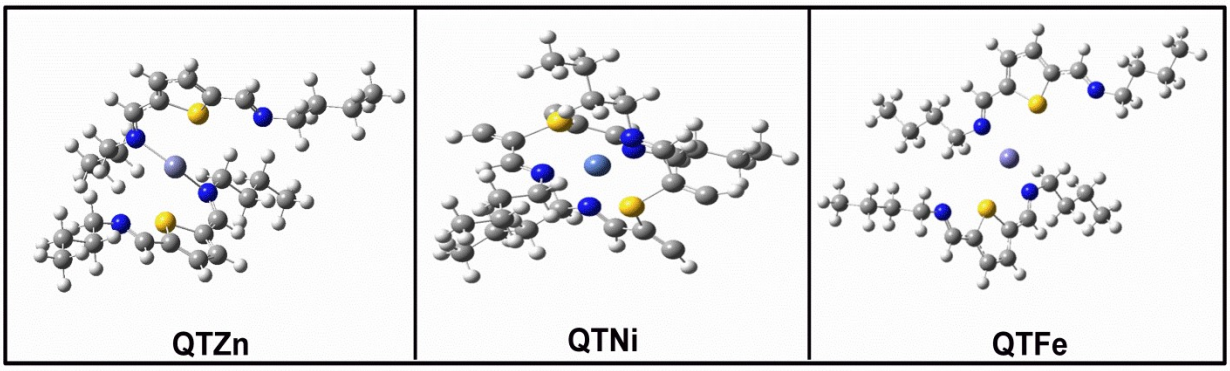

b)

	Bond Type	Bond Energy (kcal/mol)
QTZn	Zn- N	101
	Zn- S	37.3
QTNi	Ni- N	87.2
	Ni- S	52.1
QTFe	Fe- N	30.4
	Fe- S	6.1

c)

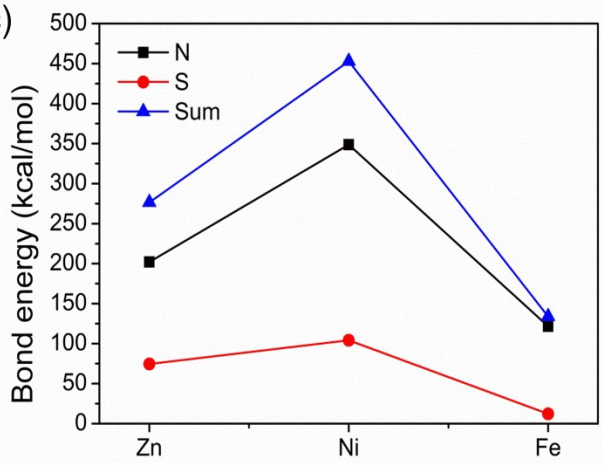

Fig. S5 DFT calculations of the bond strengths of the metallopolymers: a) Optimized molecular structures used; b) Calculated bond energies; c) Comparison of bond energies of samples: sum bond energies (blue line) were calculated based on the total maximum number of bonds. For instance, in the case of QTFe, it is the total of the energies of four Fe-N and two Fe-S bonds (the table on the other hands shows the energy values of a single bond).

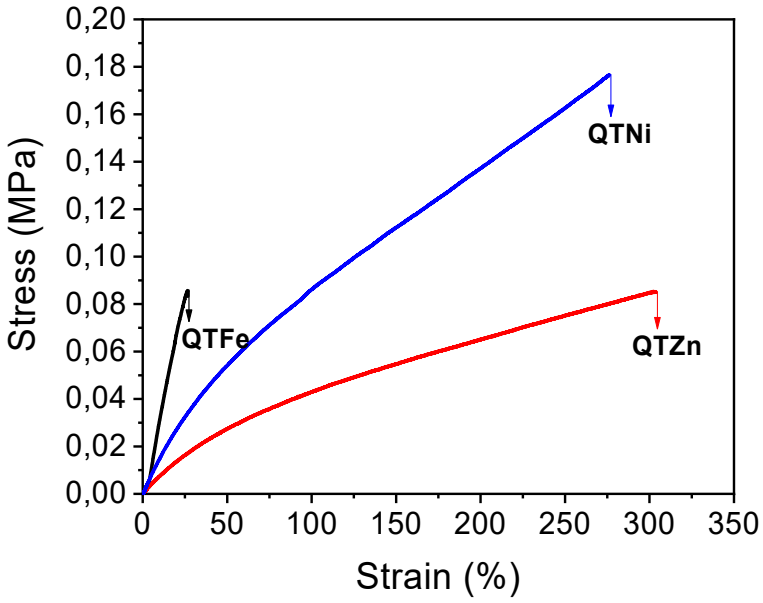

Fig. S6 Stress-strain curves of the metallopolymer elastomers. Ni complex resulted in highest mechanical strength. Stress-strain curves of the metallopolymer elastomers. Ni complex resulted in the highest mechanical strength, as seen in the UTS.

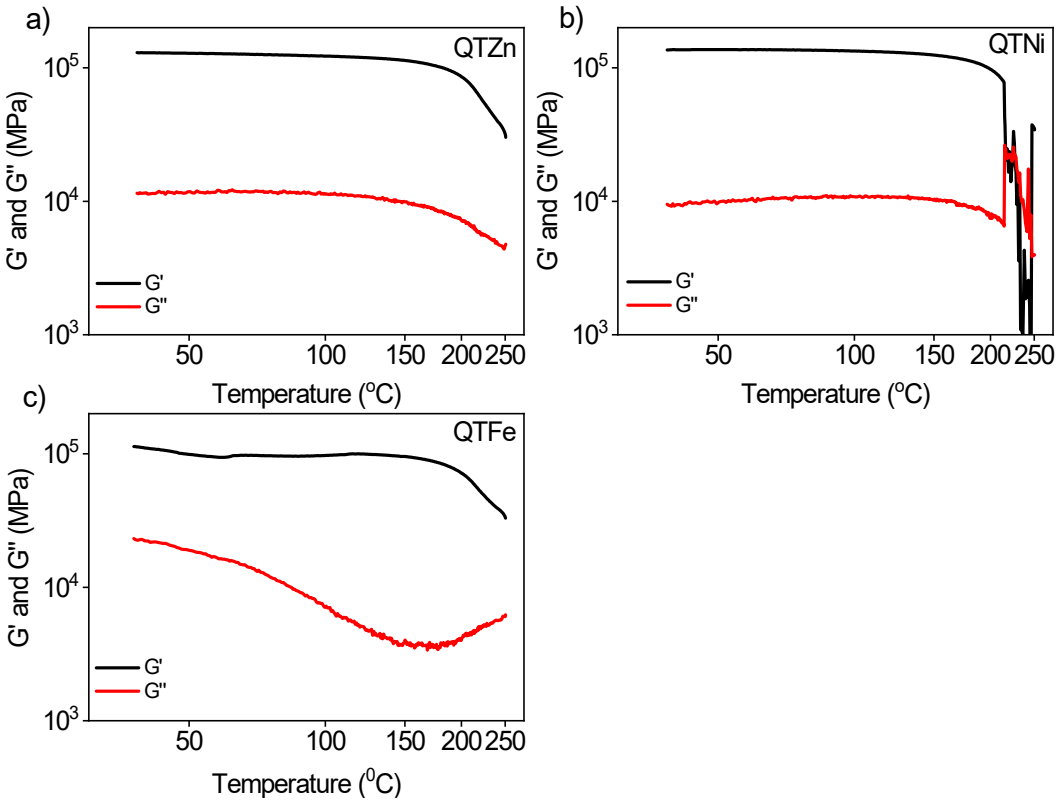

Fig. S7 Rheological temperature sweep tests at frequency 1Hz in parallel plate for: a) QTZN, b) QTNi; and c)QTFe. Figure indicates that no T-dependent crossover related to healing (G’’>G’) was observed for any polymer before terminal flow at high temperatures >250 °C.

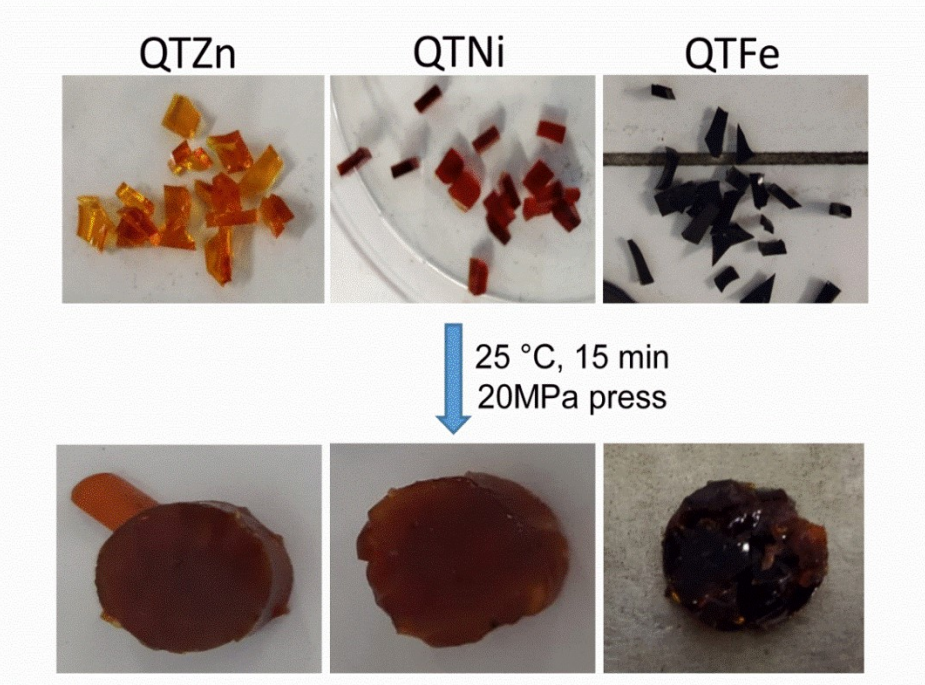

Fig. S8 Recycling behavior of the polymers. Although QTZn and QTNi can be fully recycled under pressure at room temperature, QTFe cannot.

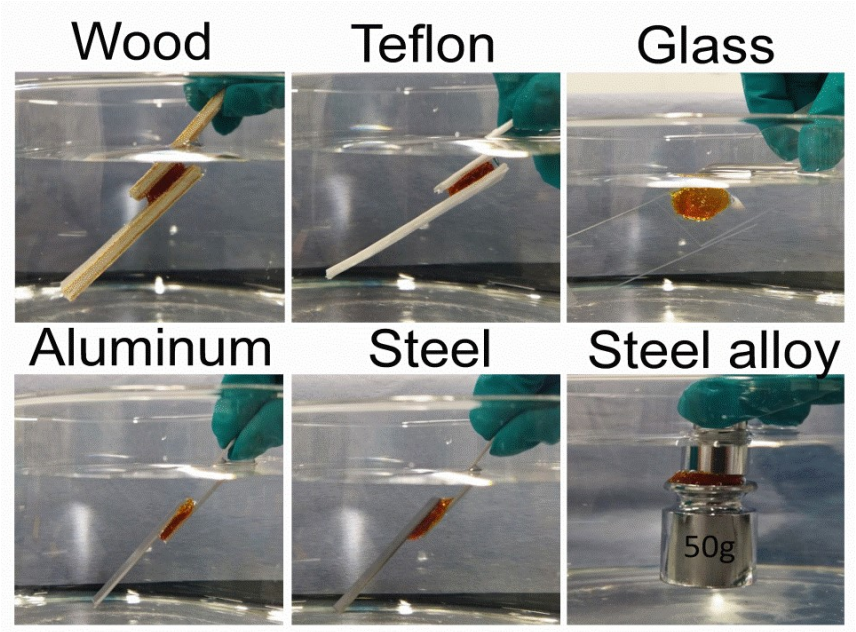

Fig. S9 Adhesion of QTNi on various hydrophilic and hydrophobic surfaces underwater. QTNi can adhere to all surfaces underwater and carry 50g of weight.

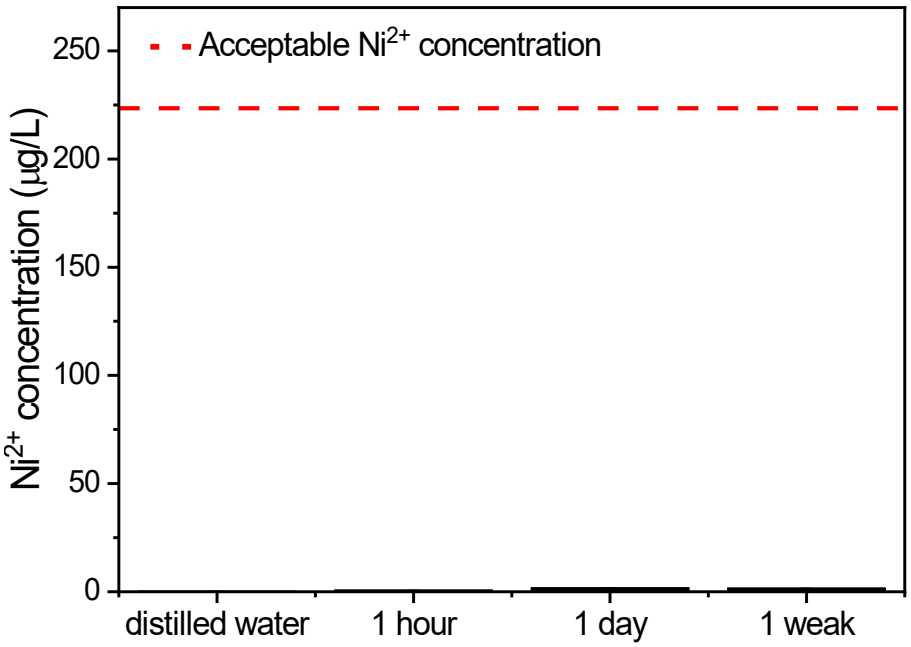

Fig. S10 Concentration of Ni^{2+} ion in water after different leaching times with a liquid/solid ratio of 150 L/kg. Leaching stabilizes after one day at a Ni^{2+} concentration in water significantly below the established acceptable Ni^{2+} concentration in drinking water for humans.

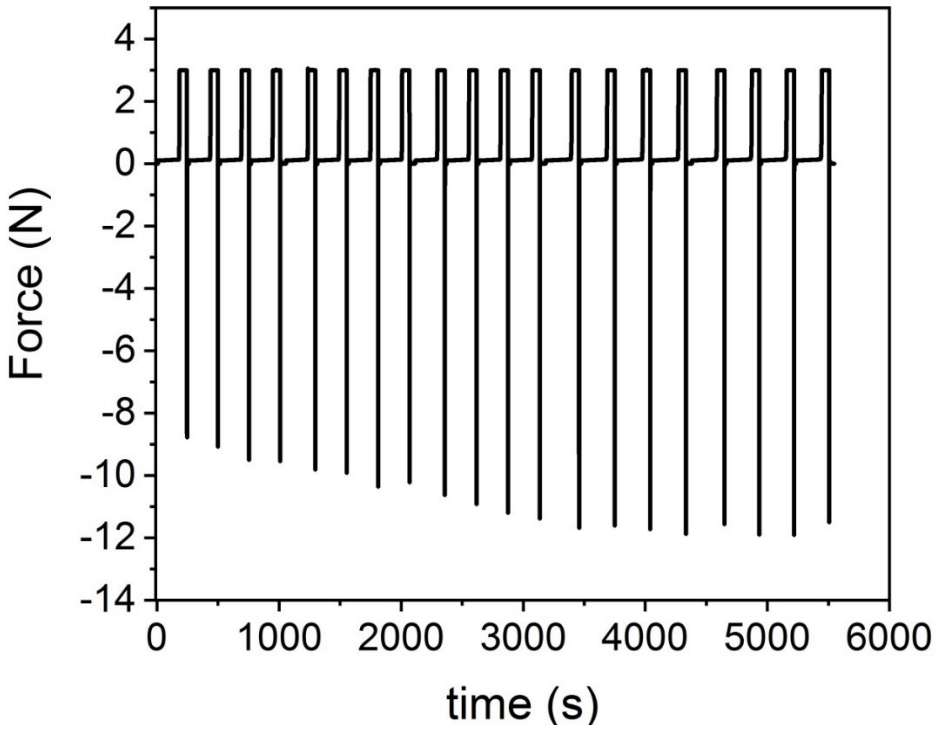

Fig. S11 Example of cyclic adhesion test curve of QTNi on glass surface. Contact force was set at 2N. Plot shows not effect of the cyclic testing on adhesion after 11 cycles and an overall minimal drift.

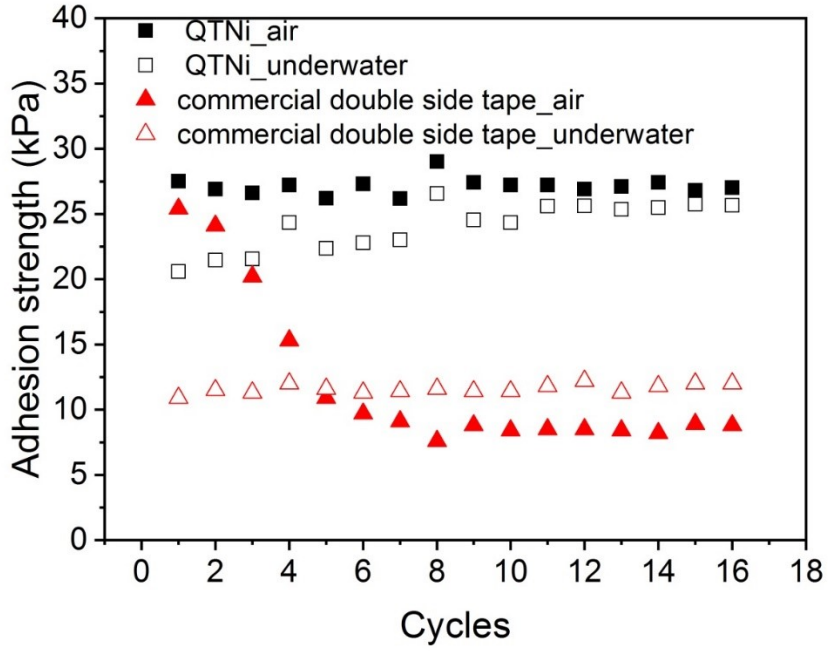

Fig. S12 Adhesion strength on aluminium measured in adhesive cycling test (16 cycles) comparing QTNi and a commercial double-side solid adhesive tested in air and underwater. Figure shows two times higher adhesion for the novel underwater adhesive and a residual adhesion for the commercial solid adhesive.

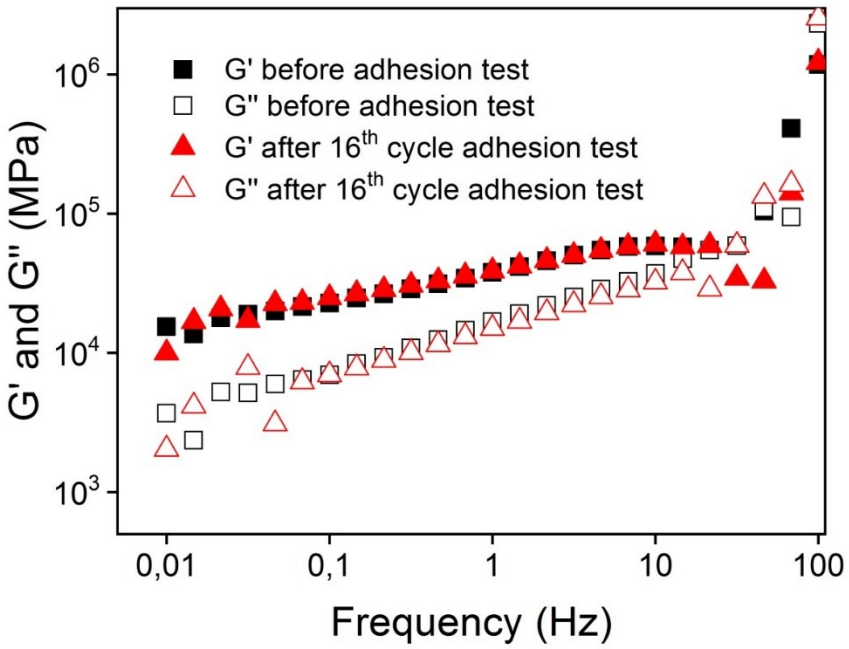

Fig. S13 Frequency sweep rheological test of QTNi before and after adhesion test (immersion in water and after 16 adhesion cycles). The test shows there are no measurable structural changes observed in the polymer due to the adhesion test or/and exposure to water.

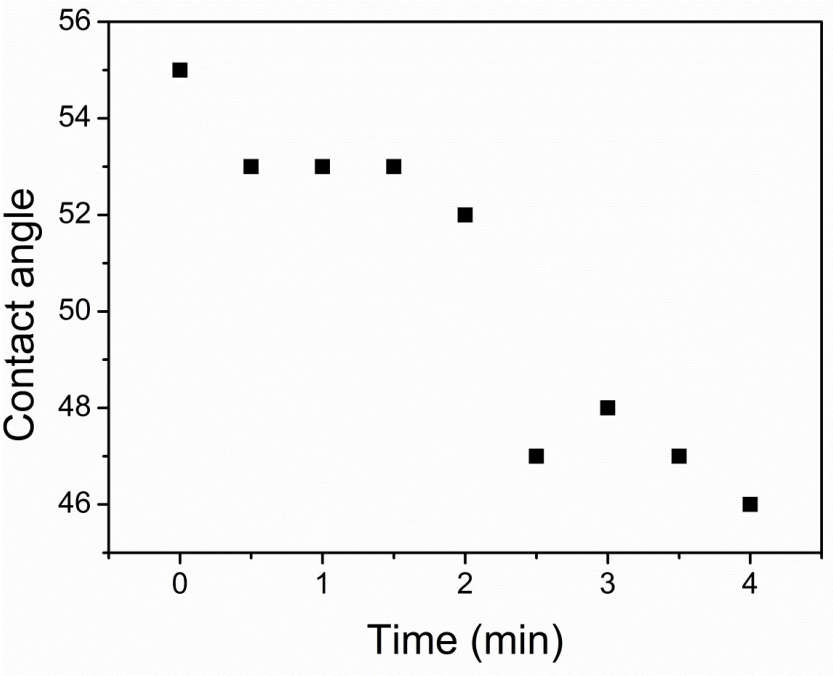

Fig. S14 Contact angle of QTNi with olive oil. Test shows how polymer chain reorientation also rapidly takes place with non-polar liquids to increase affinity to the oil (similarly as polymer adapts to increase affinity to water).

Supplementary movies

Movie S1. Self-healing experiment of QTZn under water.

Movie S2. Demonstration of reversible adhesion of QTNi to Teflon underwater. The polymer rapidly adheres to Teflon under water. The adhesive interface is broken in air upon lateral shear force and polymer-substrate interface fracture crack opening.

Movie S3. Underwater adhesion test of QTNi on and aluminium alloy surface.

The data underlying this study are openly available via a link to 4TU.ReaserchData online repository (http:doi.org//10.4121/7ad0b47d-5dcf-4918-af1e-9fd7b082de07).

References

1. Brown, I. D. 2009. “Recent Developments in the Methods and Applications of the Bond Valence Model”, Chem. Rew., 109, 6858-6919.

2. N. E. Brese and M. O'Keeffe, *Acta Crystallographica Section B Structural Science*, 1991, **47**, 192-197.

3. P. J. Flory and J. Rehner, *The Journal of Chemical Physics*, 1943, **11**, 521-526.